ADVANCED FUNCTIONAL MATERIALS
www.afm-journal.de

Comparison of Two D–A Type Polymers with Each Being Fluorinated on D and A Unit for High Performance Solar Cells

*Jea Woong Jo, Seunghwan Bae, Feng Liu, Thomas P. Russell, and Won Ho Jo**

For the purpose of investigating the effect of fluorination position on D–A type conjugated polymer on photophysical and photovoltaic properties, two types of fluorinated polymere are synthesized, HF with fluorination on electron-donating unit and FH with fluorination on electron-accepting unit. Compared to non-fluorinated polymer, fluorinated polymers exhibit deeper HOMO energy levels without change of bandgap and stronger vibronic shoulder in UV–visible absorption, indicating that fluorination enhances intermolecular interaction. HF with fluorinated D unit exhibits well-developed fibril network, low bimolecular recombination and high hole mobility, which lead a high PCE of 7.10% in conventional single-junction solar cells, which is higher than the PCE (6.41%) of FH with fluorinated A unit. Therefore, this result demonstrates that fluorination on electron-donating unit in D–A polymers could be a promising strategy for achieving high performance polymer solar cells.

1. Introduction

Electronic energy level engineering of conjugated polymers including low bandgap for harvesting a wide range of solar spectrum for high short circuit current (J_{SC}),[1] deep highest occupied molecular orbital (HOMO) energy level for high open circuit voltage (V_{OC})[2] and sufficient offset of lowest unoccupied molecular orbital (LUMO) energy level between polymer donor and fullerene acceptor[3] is a key strategy to achieve high performance polymer solar cells. Over the past decade, alternating conjugated copolymers composed of electron-donating (D) and electron-accepting (A) units have been considered the most promising molecular structure for high performance polymer solar cells, because energy levels of the copolymers can be effectively tuned with a proper combination of D and A units.[4] Moreover, molecular characteristics of D–A polymers such as molecular chain ordering, dipole moment, planarity of backbone, solubility in organic solvents and miscibility with fullerene can also be fine-tuned by modifying each of D and A building blocks separately.[5]

Among a wide variety of D–A polymers, polymers with fluorinated building block have recently attracted great interest because high power conversion efficiencies (PCEs) over 7% have been achieved by fluorination of A unit.[2a,6] Since fluorine atom has strong electron-withdrawing nature with the highest electronegativity, fluorinated polymers exhibit deeper HOMO energy levels without change of bandgap, and thus afford higher V_{OC}s than non-fluorinated ones without sacrifice of J_{SC}s. Furthermore, enhanced inter/intramolecular interaction of polymers due to strongly induced dipole in C–F bond leads to high charge carrier mobility and well-developed fibril structure in the active layer of polymer solar cells, contributing to both enhancement of J_{SC} and fill factor (FF). Until now, the effect of fluorination on D unit in D–A polymer on photovoltaic properties has scarcely been studied, while most of studies have focused on the fluorination on A unit in the copolymers.

In this work, we synthesized two kinds of D–A polymers with each being fluorinated on A and D unit, where quaterthiophene (QT) and benzothiadiazole (BT) are used as D and A unit, respectively, in order to investigate the effect of fluorination position on photophysical properties of polymers and their device performances of polymer solar cells. Although the fluorination on either D or A unit effectively enhances intermolecular interaction exhibiting strong vibronic shoulder in UV–visible absorption spectra, and lowers both LUMO and HOMO energy levels retaining a low bandgap of 1.58 eV, the polymer with fluorinated D unit exhibits a PCE of 7.10% with well-developed fibril network, while the polymer with fluorinated A unit exhibits a PCE of 6.41%. Therefore it can be concluded that the fluorination on D unit in D–A polymer is a very promising and comparable to or even more effective than the fluorination on A unit for achieving high performance solar cells.

J. W. Jo, S. Bae, Prof. W. H. Jo
Department of Materials Science and Engineering
Seoul National University
1, Gwanak-ro, Gwanak-gu, Seoul 151–744, Korea
E-mail: whjpoly@snu.ac.kr
F. Liu, Prof. T. P. Russell
Department of Polymer Science and Engineering
University of Massachusetts
Amherst, MA 01003, USA

DOI: 10.1002/adfm.201402210

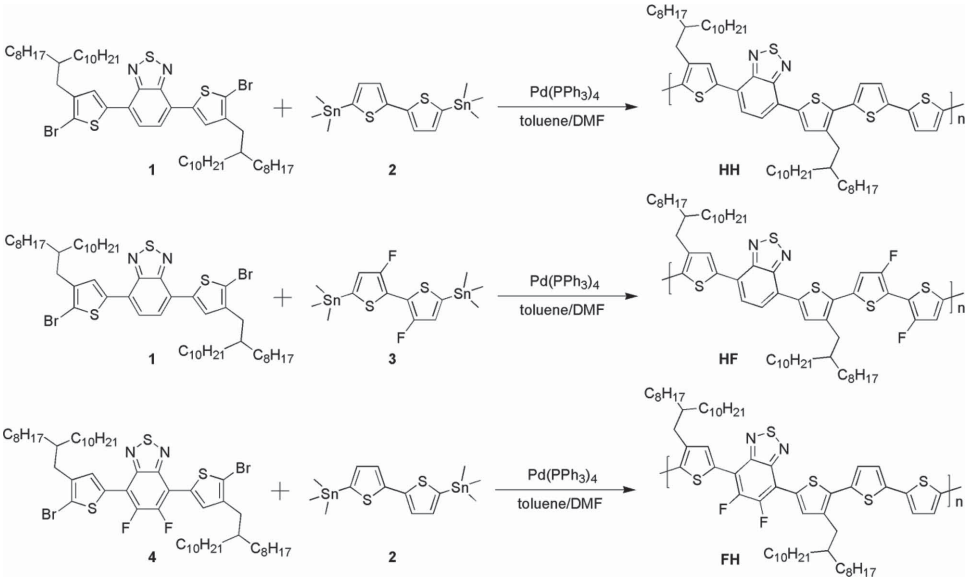

Scheme 1. Synthesis of polymers.

2. Results and Discussion

A non-fluorinated D–A polymer (denoted as HH) and two different fluorinated D–A polymers (denoted as HF and FH for the copolymer with fluorinated D unit and the copolymer with fluorinated A unit, respectively) were synthesized via the Stille coupling reaction in toluene/DMF with $Pd(PPh_3)_4$ as a catalyst, as shown in **Scheme 1**. When the number average molecular weights (M_n) and polydispersity indexes (PDI) of polymers were measured by gel permeation chromatography (GPC), as listed in **Table 1**, it reveals that all polymers have sufficient molecular weight (>40 kDa) not as to significantly affect their photovoltaic performances. Synthesized polymers are highly soluble in common organic solvents such as chloroform, chlorobenzene and dichlorobenzene at room temperature. All polymers are thermally stable up to 400 °C (see Figure S1, Supporting Information). When the melting and crystallization temperatures are measured by a differential scanning calorimetry, the melting and crystallization temperatures of fluorinated polymers (HF and FH) are higher than non-fluorinated one (HH) (see Figure S2, Supporting Information).

When UV–visible absorption spectra of the D–A polymers in chloroform solution and film state are compared, as shown in **Figure 1**, an identical onset of absorption spectrum is observed at 785 nm for all polymers, corresponding to a bandgap of 1.58 eV. While the absorption spectrum of HH in film state is red-shifted as compared to that in solution, the absorption spectra of HF and FH in solution are similar to those of film state, respectively, indicating that fluorinated polymers already aggregate in solution due to strong intermolecular interaction. Furthermore, the two fluorinated polymers (HF and FH) exhibit stronger vibronic shoulder around 690 nm and higher absorptivity than HH, because the substitution of fluorine atom enhances interaction between polymer chains. Hence, well-developed crystallites of the fluorinated polymers due to strong interchain interaction are expected to afford higher photocurrents. When electrochemical properties of polymer films are measured by cyclic voltammetry, as shown in **Figure 2**, HH, HF, and FH have the HOMO energy levels of –5.31, –5.42, and –5.38 eV, respectively, indicating that the fluorine atom substitution can effectively lower the HOMO energy level of polymer, particularly more effective when the D unit is fluorinated. Therefore, the device fabricated from HF is expected to exhibit the highest V_{OC}, because V_{OC} is proportional to the difference between the HOMO energy level of donor polymer and the LUMO energy level of fullerene acceptor.[2b]

Table 1. Characteristics of polymers.

Polymer	M_n [kg/mol]	PDI	$E_{g,opt}$ [a)] [eV]	HOMO [eV]	LUMO [b)] [eV]
HH	42	1.45	1.58	–5.31	–3.73
HF	58	1.92	1.58	–5.42	–3.84
FH	54	1.69	1.58	–5.38	–3.80

[a)] Determined from the onset of UV–Vis absorption spectra.
[b)] $E_{g,opt}$ + HOMO.

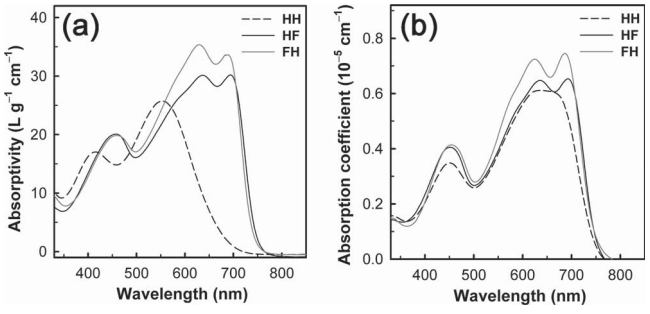

Figure 1. UV–Visible absorption spectra of polymers in a) $CHCl_3$ solution and b) film state.

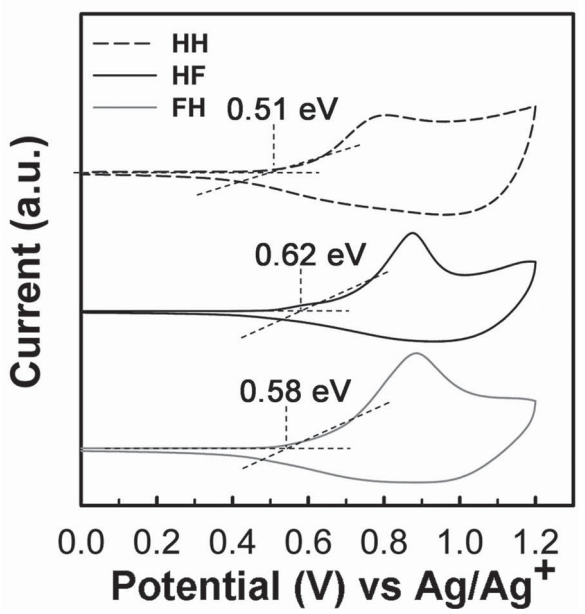

Figure 2. Cyclic voltammograms of polymers.

The torsion angle and orbital distribution of fluorinated polymers simulated by the density functional theory (DFT) are shown in Figure S3 (Supporting Information), and the calculated data are summarized in Table S1. Since fluorine atom has small size (van der Waals radius, $r = 1.35$ Å) and thus may not significantly induce steric hindrance, all polymers exhibit nearly planar structure, leading to improved intermolecular interaction between polymer chains with extended π-conjugation. The HOMO and LUMO energy levels of both fluorinated polymers are well localized on the D and A unit, respectively, and also exhibit similar orbital distribution and energy levels, indicating that intramolecular charge transfer takes place upon excitation regardless of the fluorination position. It has recently been demonstrated that a large dipole change from ground to excited state ($\Delta\mu_{ge}$) facilitates exciton dissociation and generation of charge-separated state.[7] When dipole moments were calculated for repeating units of the three polymers, as listed in **Table 2**, FH (26.3 D) and HF (24.3 D) have a lager $\Delta\mu_{ge}$ than HH (19.7 D), predicting that the solar cell devices with fluorinated polymers exhibit higher J_{SC} values.

The polymer solar cells were fabricated with the conventional device configuration of ITO/PEDOT:PSS/polymer:$PC_{71}BM$/Ca/Al. Current density–voltage (J–V) characteristics under AM 1.5G illumination are shown in **Figure 3**a

Table 2. Dipole moments of repeating units calculated by time-dependent DFT.

Polymer	μ_g [D]	μ_{ex} [D]	$\Delta\mu_{ge}$ [a)] [D]
HH	3.26	22.5	19.7
HF	2.97	22.5	24.3
FH	2.82	23.5	26.3

[a)] $\Delta\mu_{ge} = [(\mu_{gx} - \mu_{ex})^2 + (\mu_{gy} - \mu_{ey})^2 + (\mu_{gz} - \mu_{ez})^2]^{1/2}$

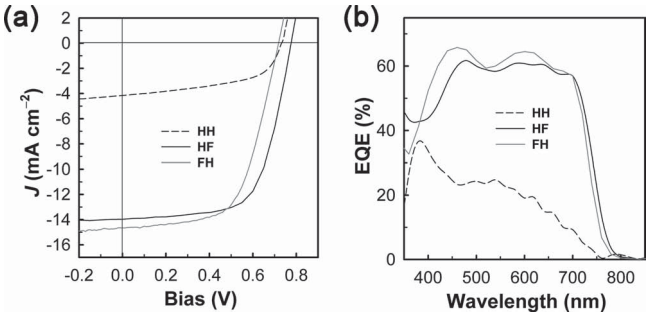

Figure 3. a) J–V curves and b) EQE spectra of polymer/$PC_{71}BM$ solar cells.

and relevant photovoltaic properties are summarized in **Table 3**. When the blend ratio of polymer to $PC_{71}BM$ was varied, the optimized ratio was 1:1. It is expected that both fluorinated polymers (HF and FH) exhibit larger J_{SC} and higher fill factor (FF) than non-fluorinated one (HH) due to higher absorption coefficient, enhanced interchain interaction and higher $\Delta\mu_{ge}$ of fluorinated polymers while HF exhibits higher V_{OC}s than the other two polymers becuase of the deepest HOMO energy level. Consequently, HF and FH exhibit high PCEs of 7.10% and 6.41%, respectively, while HH exhibits a low PCE of 1.64%, indicating that the fluorination on D unit in D–A polymer is a competitive strategy for developing high performance polymer solar cells as compared to the fluorination on A unit. It should be noted here that addition of additives does not enhance the photovoltaic performance (see Table S3). When external quantum efficiencies (EQEs) of devices were measured under monochromatic light, as shown in Figure 3b, both fluorinated polymers exhibit higher EQEs (about 60%) than that of HH in the range of 450–720 nm, consistent with higher J_{SC} of solar cells with fluorinated polymers than the solar cell with non-fluorinated one.

Intensity-dependent photocurrent (J_{ph}) were measured between 0.4 and 2.5 sun and the relative J_{ph} at $V = 0$ V are plotted against light intensity (P_{light}) in **Figure 4**a. The relationship between J_{ph} and P_{light} can be represented by a power law equation: $J_{ph} \propto (P_{light})^{\alpha}$, where α is recombination parameter.[8] Since $\alpha = 1$ corresponds to the absence of photocurrent loss due to bimolecular recombination, higher α values for HF (0.97) and FH (0.96) than the value for HH (0.93) indicate that bimolecular recombination is more suppressed in active layers with fluorinated polymers than the active layer with non-fluorinated polymer while the fluorinated position does not affect the recombination. When hole mobilities were measured from dark J–V curve of hole-only device by using the space charge limited current (SCLC) model, as shown in Figure 4b, HF/$PC_{71}BM$ (1.26×10^{-3} cm^2 V^{-1} s^{-1}) and FH/$PC_{71}BM$ (1.16×10^{-3} cm^2 V^{-1} s^{-1}) exhibit higher mobilities than HH/$PC_{71}BM$ (5.24×10^{-4} cm^2 V^{-1} s^{-1}), implying that the charge pathway are well formed in the active layers of fluorinated polymers. The crystal structure and its orientation of fluorinated polymers were investigated by the grazing-incidence wide angle X–ray scattering (GIWAXS). All blend films of polymer and $PC_{71}BM$ show only (h00) reflections in the out-of-plane (q_z) direction, as shown in **Figure 5**, indicating that polymers have preferentially edge-on orientation on the substrate. Since

Table 3. Photovoltaic properties of devices under standard AM 1.5G illumination.

Polymer	Polymer: $PC_{71}BM$ [w/w]	Thickness [nm]	$\mu_{h,SCLC}$ [cm^2/V s]	V_{OC} [V]	J_{SC} [mA/cm^2]	FF [%]	$PCE_{max}(_{aver})$ [%]
HH	1:1	90	5.24×10^{-4}	0.73	4.15	54	1.64(1.45)
HF	1:1	100	1.26×10^{-3}	0.78	14.0	65	7.10(6.70)
FH	1:1	90	1.16×10^{-3}	0.72	14.6	61	6.41(6.15)

the (100) peaks of HH, HF and FH are observed at q_z = 0.36, 0.33 and 0.33 $Å^{-1}$, corresponding to the interchain distance of 17.5, 19.0 and 19.0 Å, respectively, the inter-chain distances of fluorinated polymers are larger than the non-fluorinated one. Another feature to be noted from GIWAXS is that the two fluorinated polymers exhibit the (010) reflection at q_{xy} = 1.7 $Å^{-1}$ corresponding to the π–π stacking distance of 3.70 Å, while HH does not show discernibly the (010) peak, indicating that fluorinated polymer chains are better packed in π–π direction.

The morphologies of polymer/$PC_{71}BM$ blend films as observed by transmission electron microscope (TEM) reveal that both the blend films of HF:$PC_{71}BM$ and FH:$PC_{71}BM$ exhibit well-developed interconnected network with nanoscale fibril structure, as shown in **Figure 6**. In a previous report,[9] D–A polymers with fluorinated D unit showed poor miscibility with PCBM and thus large phase separation between polymer and PCBM, which is not beneficial for generation of charge carriers. But, this is contradictory to our system, because HF with fluorinated D unit in our system shows well-developed interconnected network strucute with nanoscale phase separation.

3. Conclusion

We designed and synthesized two types of fluorinated D–A polymers with each being fluorinated on D and A unit, where QT and BT used as D and A units, respectively. Compared to non-fluorinated polymer, both fluorinated polymers have deeper HOMO energy levels without change of optical bandgap and exibit stronger vibronic shoulder in optical spectrum. The HF polymer with fluorinated D unit exhibits higher PCE of 7.10% than FH with fluorinated A unit (PCE = 6.41%). Since the HF polymer exhibits low bimolecular recombination, high hole mobility and well-developed fibril network, it is conclusive that the fluorination on D unit in D–A polymer could be a promising method for achieving high performance polymer solar cells.

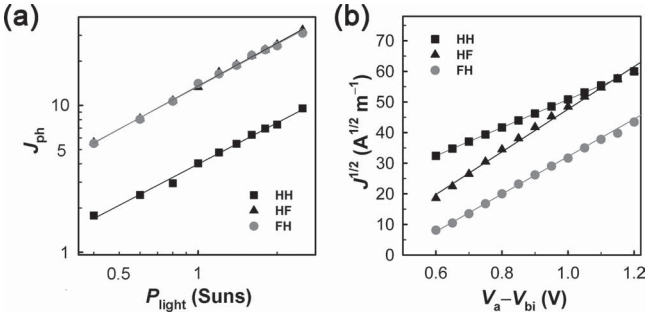

Figure 4. a) Plot of relative J_{ph} vs light intensity as measured at V = 0 V; b) dark J–V characteristics of polymer/$PC_{71}BM$ blends with hole-only device, where the solid lines represent the best linear fit of the data points.

4. Experimental Section

Materials: 4,7-Bis[5-bromo-4-(2-octyldodecyl)thiophene-2-yl]-benzo[*c*][1,2,5]thiadiazole (**1**),[4f] 5,5'-bis(trimethyl-stannyl)-2,2'-bithiophene (**2**),[10] 5,5'-bis(trimethylstannyl)-3,3'-difluoro-2,2'-bithiophene (**3**)[11] and 5,6-difluoro-4,7-bis[5-bromo-4-(2-octyldodecyl)thiophene-2-yl]-benzo[*c*][1,2,5]thiadiazole (**4**),[12] were synthesized by following the methods reported in the literatures. Poly(3,4-ethylenedioxy-thiophene):poly(styrene-sulfonate) (PEDOT:PSS) (Clevios P VP AI 4083) was purchased from H. C. Stark and passed through a 0.45 μm PVDF syringe filter before spin-coating. [6,6]-Phenyl-C_{71}-butyric acid methyl ester ($PC_{71}BM$) was obtained from Nano-C. All reagents were purchased from Sigma-Aldrich unless specified and used as received.

Synthesis of Polymers: The polymer HH was synthesized by following the method reported in the literature.[4f] The polymer HF was synthesized as follows: the compounds **1** (120 mg, 0.12 mmol) and **3** (64 mg, 0.12 mmol) were dissolved in a mixture of toluene (10 mL) and DMF (1 mL). After the solution was flushed with N_2 for 20 min, 20 mg of $Pd(PPh_3)_4$ was added. The reaction mixture was then refluxed for 3 days. After being cooled to room temperature, the mixture was poured into methanol. The crude product was filtered through a Soxhlet thimble and then subjected to Soxhlet extraction successively with methanol, ethyl acetate, hexane and chloroform. The chloroform fraction was precipitated into methanol to afford the product as a dark green solid (85 mg, 67%). FH was synthesized by following the same procedure as used in the synthesis of HF: The compound **4** (139 mg, 0.13 mmol) and **2** (65 mg, 0.13 mmol) were used as monomers, and a dark green solid was obtained as a product (100 mg, 72%).

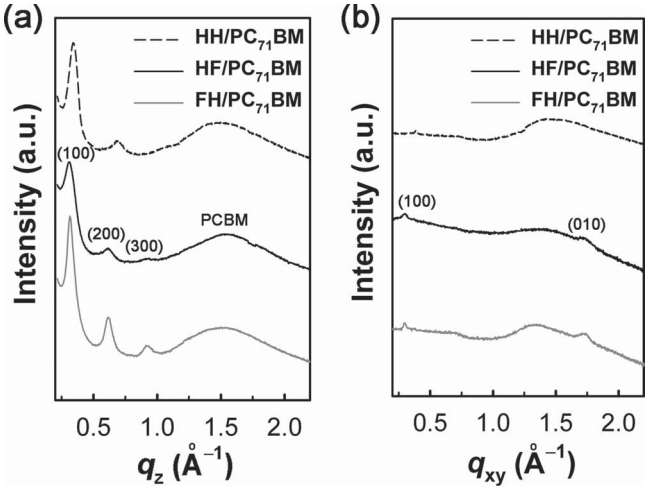

Figure 5. a) q_z and b) q_{xy} scans of GIWAXS from thin films of polymer/$PC_{71}BM$.

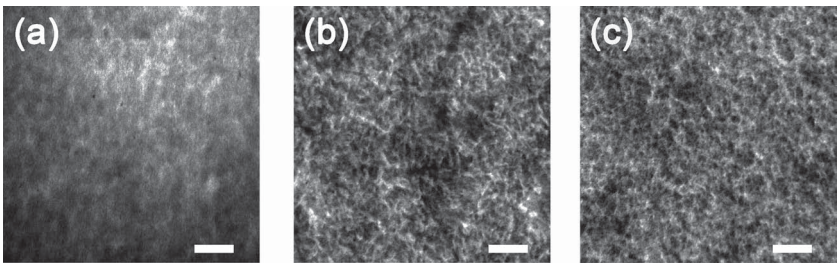

Figure 6. TEM images of a) HH/$PC_{71}BM$, b)HF/$PC_{71}BM$, and c) FH/$PC_{71}BM$ blend films. The scale bar denotes 200 nm.

Characterization: Molecular weight and its distribution of polymers were measured by GPC (Polymer Labs GPC 220) with a refractive index detector at 135 °C. 1,2,4-Trichlorobenzene was used as an eluent, and the molecular weight of polymers were calibrated by polystyrene standards. The optical absorption spectra were obtained by an UV–Visible spectrophotometer (Perkin-Elmer Lamda 25). Cyclic voltammetry were conducted on a potentiostat/galvanostat (VMP3, Biologic) in an electrolyte solution of 0.1 M tetrabutylammonium hexafluorophosphate acetonitrile. Pt wires (Bioanalytical System Inc.) were used as both counter and working electrodes, and silver/silver ion (Ag in 0.1 M $AgNO_3$ solution, Bioanalytical System Inc.) was used as a reference electrode. The HOMO energy levels of polymers were calculated by using the equation: HOMO(eV) = $-[E_{ox} - E_{1/2}$(ferrocene) + 4.8], where E_{ox} is the onset oxidation potential of the polymer and $E_{1/2}$(ferrocene) is the onset oxidation potential of ferrocene vs Ag/Ag^+. DFT calculations at the B3LYP/6–31G(d,p) level were carried out on Gaussian 09. Dipole moments in ground and excited states were calculated with time-dependent DFT.[8a] Thermogravimetric analysis was carried out at a heating rate of 10 °C min^{-1} under nitrogen atmosphere using a thermogravimetric analyzer (TA 2050, TA Instruments). Melting and crystallization temperatures were measured by heating and cooling the sample from 20 to 350 °C at a scan rate of 10 °C min^{-1} using a differential scanning calorimeter (TA Instruments, 2920 Modulated DSC).

Device Fabrication and Testing: The polymer solar cells were fabricated with a standard device configuration of glass/ITO/PEDOT:PSS/polymer:$PC_{71}BM$/Ca/Al. PEDOT:PSS was spin-coated with 40 nm thickness on the ITO-coated glass and annealed at 150 °C for 30 min. The blend solution of 2 wt% in o-dichlorobenzene was spin-coated on the top of the PEDOT:PSS layer at 800–1000 rpm for 40 s. The film thickness of the active layer was measured by atomic force microscopy (Nano Xpert II, EM4SYS). Calcium (20 nm) and aluminum (100 nm) was thermally evaporated on the top of the active layer under vacuum (<10^{-6} Torr). The effective area of the cell was 0.1 cm^2. The *J–V* characteristics were measured with a Keithley 4200 source-meter under AM 1.5G (100 mW/cm^2) simulated by a Newport-Oriel solar simulator. The light intensity was calibrated using a NREL-certified photodiode prior to each measurement. The EQE was measured using a lock-in amplifier with a current preamplifier (K3100, Mac Science Co.) under short circuit current state with illumination of monochromatic light. The morphologies of polymer/$PC_{71}BM$ blend films were observed by TEM (JEM-1010, JEOL). The SCLC *J–V* curves were obtained in the dark using hole-only devices (ITO/PEDOT:PSS/polymer:$PC_{71}BM$/Au), and hole mobilities were calculated using the Mott-Gurney square law, $J = (9/8)\varepsilon_0 \varepsilon_r \mu (V^2/L^3)$, where ε_0 is vacuum permittivity, ε_r is the dielectric constant of polymer, μ is the charge carrier mobility, V is the effective applied voltage, and L is the thickness of the film. GIWAXS scans were obtained at the Advanced Light Source at the Lawrence Berkeley National Laboratory. The wavelength of X–ray used was 1.240 Å, and the scattered intensity was detected by PILATUS 1M detector.

Supporting Information

Supporting Information is available from the Wiley Online Library or from the author.

Acknowledgements

The authors thank the Ministry of Education, Science and Technology (MEST), Korea for financial support through the Global Research Laboratory (GRL) program. T.P.R. and F.L. also acknowledge the support of the US Department of Energy through the Energy Frontier Research Center.

Received: July 4, 2014
Revised: August 27, 2014
Published online: October 27, 2014

[1] a) N. Blouin, A. Michaud, M. Leclerc, *Adv. Mater.* **2007**, *19*, 2295; b) J. W. Chen, Y. Cao, *Acc. Chem. Res.* **2009**, *42*, 1709; c) E. Bundgaard, F. C. Krebs, *Sol. Energy Mater. Sol. Cells* **2007**, *91*, 954; d) D. Gendron, M. Leclerc, *Energy Environ. Sci.* **2011**, *4*, 1225; e) C. L. Chochos, S. A. Choulis, *Prog. Polym. Sci.* **2011**, *36*, 1326.

[2] a) H. Y. Chen, J. H. Hou, S. Q. Zhang, Y. Y. Liang, G. W. Yang, Y. Yang, L. P. Yu, Y. Wu, G. Li, *Nat. Photonics* **2009**, *3*, 649; b) M. D. Perez, C. Borek, S. R. Forrest, M. E. Thompson, *J. Am. Chem. Soc.* **2009**, *131*, 9281; c) A. Maurano, R. Hamilton, C. G. Shuttle, A. M. Ballantyne, J. Nelson, B. O'Regan, W. Zhang, I. McCulloch, H. Azimi, M. Morana, C. J. Brabec, J. R. Durrant, *Adv. Mater.* **2010**, *22*, 4987; d) D. Veldman, S. C. J. Meskers, R. A. J. Janssen, *Adv. Mater.* **2009**, *19*, 1939.

[3] a) Y. Lee, W. H. Jo, *J. Phys. Chem. C* **2012**, *116*, 8379; b) C. J. Brabec, S. Gowrisanker, J. J. M. Halls, D. Laird, S. Jia, S. P. Williams, *Adv. Mater.* **2010**, *22*, 3839.

[4] a) J. W. Jo, S. S. Kim, W. H. Jo, *Org. Electron.* **2012**, *13*, 1322; b) H. X. Zhou, L. Q. Yang, S. C. Price, K. J. Knight, W. You, *Angew. Chem. Int. Ed.* **2010**, *49*, 7992; c) C. Y. Yu, C. P. Chen, S. H. Chan, G. W. Hwang, C. Ting, *Chem. Mater.* **2009**, *21*, 3262; d) N. Blouin, A. Michaud, D. Gendron, S. Wakim, E. Blair, R. Neagu-Plesu, M. Belletête, G. Durocher, Y. Tao, M. Leclerc, *J. Am. Chem. Soc.* **2008**, *130*, 732; e) K. H. Ong, S. L. Lim, H. S. Tan, H. K. Wong, J. Li, Z. Ma, L. C. H. Moh, S. H. Lim, J. C. De Mello, Z. K. Chen, *Adv. Mater.* **2011**, *23*, 1409; f) I. Osaka, M. Shimawaki, H. Mori, I. Doi, E. Miyazaki, T. Koganezawa, K. Takimiya, *J. Am. Chem. Soc.* **2012**, *134*, 3498; g) J.-F. Jheng, Y.-Y. Lai, J.-S. Wu, Y.-H. Chao, C.-L. Wang, C.-S. Hsu, *Adv. Mater.* **2013**, *25*, 2445; h) R. S. Ashraf, B. C. Schroeder, H. A. Bronstein, Z. Huang, S. Thomas, R. J. Kline, C. J. Brabec, P. Rannou, T. D. Anthopoulos, J. R. Durrant, I. McCulloch, *Adv. Mater.* **2013**, *25*, 2029.

[5] a) E. H. Jung, W. H. Jo, *Energy Environ. Sci.* **2014**, *7*, 650; b) E. G. Wang, J. Bergqvist, K. Vandewal, Z. F. Ma, L. T. Hou, A. Lundin, S. Himmelberger, A. Salleo, C. Müller, O. Inganäs, F. L. Zhang, M. R. Andersson, *Adv. Energy Mater.* **2013**, *3*, 806; c) L. Q. Yang, H. X. Zhou, W. You, *J. Phys. Chem. C* **2010**, *114*, 16793; d) R. Tautz, E. Da Como, T. Limmer, J. Feldmann, H. J. Egelhaaf, E. von Hauff, V. Lemaur, D. Beljonne, S. Yilmaz, I. Dumsch, S. Allard, U. Scherf, *Nat. Commun.* **2012**, *3*; e) J. W. Jung, J. W. Jo,

F. Liu, T. P. Russell, W. H. Jo, *Chem. Commun.* **2012**, *48*, 6933; f) Y. Chen, C. Chang, Y. Cheng, C. Hsu, *Chem. Mater.* **2012**, *24*, 3964; g) L. Fang, Y. Zhou, Y. Yao, Y. Diao, W. Lee, A. L. Appleton, R. Allen, J. Reinspach, S. C. B. Mannsfeld, Z. Bao, *Chem. Mater.* **2013**, *25*, 4874; h) S. Subramaniyan, H. Xin, F. S. Kim, S. Shoaee, J. R. Durrant, S. A. Jenekhe, *Adv. Energy Mater.* **2011**, *1*, 854.

[6] a) H. X. Zhou, L. Q. Yang, A. C. Stuart, S. C. Price, S. B. Liu, W. You, *Angew. Chem. Int. Ed.* **2011**, *50*, 2995; b) S. C. Price, A. C. Stuart, L. Q. Yang, H. X. Zhou, W. You, *J. Am. Chem. Soc.* **2011**, *133*, 4625; c) H. C. Chen, Y. H. Chen, C. C. Liu, Y. C. Chien, S. W. Chou, P. T. Chou, *Chem. Mater.* **2012**, *24*, 4766; d) N. Wang, Z. Chen, W. Wei, Z. H. Jiang, *J. Am. Chem. Soc.* **2013**, *135*, 17060; e) Y. Yang, R. Wu, X. Wang, X. Xu, Z. Li, K. Li, Q. Peng, *Chem. Commun.* **2014**, *50*, 439; f) M. Zhang, X. Guo, S. Zhang, J. Hou, *Adv. Mater.* **2014**, *26*, 1118; g) Y. Xu, C. Chueh, H. Yip, F. Ding, Y. Li, C. Li, X. Li, W. Chen, A. K.-Y. Jen, *Adv. Mater.* **2012**, *24*, 6356.

[7] a) B. Carsten, J. M. Szarko, H. J. Son, W. Wang, L. Y. Lu, F. He, B. S. Rolczynski, S. J. Lou, L. X. Chen, L. P. Yu, *J. Am. Chem. Soc.* **2011**, *133*, 20468; b) B. S. Rolczynski, J. M. Szarko, H. J. Son, Y. Y. Liang, L. P. Yu, L. X. Chen, *J. Am. Chem. Soc.* **2012**, *134*, 4142.

[8] a) A. C. Stuart, J. R. Tumbleston, H. X. Zhou, W. T. Li, S. B. Liu, H. Ade, W. You, *J. Am. Chem. Soc.* **2013**, *135*, 1806; b) S. R. Cowan, J. Wang, J. Yi, Y. J. Lee, D. C. Olson, J. W. P. Hsu, *J. Appl. Phys.* **2013**, *113*, 154504.

[9] H. J. Son, W. Wang, T. Xu, Y. Y. Liang, Y. E. Wu, G. Li, L. P. Yu, *J. Am. Chem. Soc.* **2011**, *133*, 1885.

[10] H. H. Fong, V. A. Pozdin, A. Amassian, G. G. Malliaras, D. M. Smilgies, M. Q. He, S. Gasper, F. Zhang, M. Sorensen, *J. Am. Chem. Soc.* **2008**, *130*, 13202.

[11] J. W. Jo, J. W. Jung, H.–W. Wang, P. Kim, T. P. Russell, W. H. Jo, *Chem. Mater.* **2014**, *26*, 4214.

[12] Y. Wang, X. Xin, Y. Lu, T. Xiao, X. F. Xu, N. Zhao, X. Hu, B. S. Ong, S. C. Ng, *Macromolecules* **2013**, *46*, 9587.